Gas-Phase Molecular Halogen Formation from NaCl and NaBr Aerosols: When Are Interface Reactions Important?

Jennie L. Thomas,[†] Angel Jimenez-Aranda,[‡] Barbara J. Finlayson-Pitts,*[,†] and Donald Dabdub*[,‡]

Departments of Chemistry and Mechanical & Aerospace Engineering, University of California, Irvine, Irvine, California 92697

Received: August 30, 2005; In Final Form: November 10, 2005

Unique interface reactions at the surface of sea-salt particles have been suggested as an important source of photolyzable gas-phase halogen species in the troposphere. Many factors influence the relative importance of interface chemistry compared to aqueous-phase chemistry. The Model of Aerosol, Gas, and Interfacial Chemistry (MAGIC 2.0) is used to study the influence of interface reactions on gas-phase molecular halogen production from pure NaCl and NaBr aerosols. The main focus is to identify the relative importance of bulk compared to interface chemistry and to determine when interface chemistry dominates. Results show that the interface process involving $Cl^-_{(surf)}$ and $OH_{(g)}$ is the main source of $Cl_{2(g)}$. For the analogous oxidation of bromide by OH, gaseous Br_2 is formed mainly in the bulk aqueous phase and transferred across the interface. However, the reaction of $Br^-_{(surf)}$ with $O_{3(g)}$ at the interface is the primary source of $Br_{2(g)}$ under dark conditions. The effect of aerosol size is also studied. Potential atmospheric implications and effects of interface processes on aerosol pH are discussed.

1. Introduction

There is increasing evidence for reactions at air−water interfaces in a number of important systems, including in the atmosphere. For example, Hu and co-workers[1] reported that the uptake of Cl_2 on droplets containing Br^- was faster than expected from mass accommodation followed by dissolution and reaction in the bulk liquid. They postulated a reaction of Cl_2 with the bromide ion at the interface that contributed to an increased overall uptake of chlorine from the gas phase. Knipping and co-workers[2] proposed an interface reaction between OH and surface Cl^- to explain gas-phase Cl_2 production. In addition, Hunt et al.[3] used an interface reaction between O_3 and interfacial Br^- to explain the generation of Br_2 in the dark. Such reactions are plausible, given theoretical evidence for ions at interfaces,[2−14] predicted enhancements of some gases at the air−water interface,[15,16] and the results of a number of experiments[2,3,17−25] in which interface reactions had to be invoked to explain the data.

The surface propensity of ions is related to polarizability, with the interaction between a polarizable ion and the dipole moment of water at the interface competing more favorably with hydration in the bulk as the polarizability of the ion increases. However, increasing polarizability, for example, of the halide ions, is also associated with decreasing oxidation potentials. As a result, the trend down the group VII ions to greater enhancement at the air−water interface, and hence increased likelihood of unique interface reactions, is accompanied by more rapid oxidation in the bulk as well. It is not therefore immediately obvious how the relative contributions of bulk versus interface chemistry will change with the nature of the ion and under what conditions reaction in the bulk or at the interface will dominate.

The halide ions are ideal for examining this issue since they are not only of intrinsic chemical interest but also are important in the atmosphere as major components of sea-salt particles[26] and particles generated from dry alkaline lakes such as the Dead Sea in Israel[27−30] and the Great Salt Lake in the United States.[31] There are a variety of chemical reactions[32−39] that convert halide ions into gas-phase halogen compounds that generate halogen atoms upon photolysis. Because of their high reactivity, halogen atoms have the potential to impact ozone levels in the troposphere.[40−46] Thus, chlorine atoms react with organic compounds[47−49] even more rapidly that does OH, setting off the well-known volatile organic compound (VOC)−NO_x chemistry[26] that leads to ozone formation in the lower troposphere.[46] Bromine atoms, however, react very slowly with many organics,[49] so that their reaction with O_3 tends to dominate, leading to ozone destruction. Chain reactions of bromine involving interactions between the gas phase and halide ions in the snowpack such as reactions 1−4 amplify this effect and are believed to be responsible for the rapid loss of ozone at ground level in the Arctic at polar sunrise[50−61]

$$Br_2 + h\nu \rightarrow 2Br \quad (1)$$

$$Br + O_3 \rightarrow BrO + O_2 \quad (2)$$

$$BrO + HO_2 \rightarrow HOBr + O_2 \quad (3)$$

$$HOBr + Br^-_{(snowpack)} \xrightarrow{H^+} Br_2 + H_2O \quad (4)$$

Because of the contributions of halogen chemistry in determining ozone and other trace species in the troposphere, elucidating the roles of interface and bulk chemistry in generating photolyzable halogen gases is important. We report here the application of a revised version of the Model of Aerosol, Gas, and Interfacial Chemistry (MAGIC 2.0) to examine the reactions of chloride and bromide ions with OH and O_3. The

* Authors to whom correspondence should be addressed. Phone: (949) 824-7670 (B.J.F.-P.); (949) 824-6126 (D.D.). Fax (949) 824-3168 (B.J.F.-P.); (949) 824-8585 (D.D.). E-mail: bjfinlay@uci.edu; ddabdub@uci.edu.

[†] Department of Chemistry.

[‡] Department of Mechanical & Aerospace Engineering.

10.1021/jp054911c CCC: $33.50
Published on Web 01/06/2006

TABLE 1: List of Species Included in the Model[a]

group	gas-phase species	aqueous-phase species
O	$O(^1D)$, $O(^3P)$, **O_2**,**O_3**, **OH**, **HO_2**, **H_2O_2**, H_2O	$O(^3P)$, **O_2**, **O_3**, **OH**/O^-, **HO_2**/O_2^-, **H_2O_2**/HO_2^-, HO_3, O_3^-, H^+/ OH^-
Br	Br, **Br_2**, BrO, **HOBr**, **HBr**	Br, **Br_2**, Br_2^-, **HBr**/Br^-, **HOBr**/BrO^-, Br_2O_4, Br_3^-, BrO, BrO_2, $HBrO_2$/BrO_2^-, BrO_3^-, $HOBr^-$
Cl	**Cl**, **Cl_2**, ClO, OClO,ClOO, **Cl_2O**, Cl_2O_2, **HOCl**, **HCl**	Cl, **Cl_2**, Cl_2^-, **HCl**/Cl^-, **HOCl**/ClO^-, **Cl_2O**, HOClH/$HOCl^-$
CO_2	CO_2	**H_2CO_3**/HCO_3^-/CO_3^{-2}, HCO_3/CO_3^-
other	N_2	Na^+

[a] Species in bold are transferred between the gas and the aqueous phase.

model includes an unique approach that couples diffusion, interface reaction, and mass accommodation coefficients with an explicit treatment of gas- and aqueous-phase chemistry. The goal is to understand the factors that determine the relative importance of bulk compared to interface chemistry in the most simple chloride and bromide systems represented by deliquesced aerosols of NaCl or NaBr. While salt particles in the atmosphere are comprised of mixtures of chloride, bromide, and other anions, leading to interhalogen chemistry in the real atmosphere, using the single-component particles as a model allows a quantitative examination of the factors governing bulk versus interface chemistry. Such understanding is a prerequisite to probing more complex systems.

2. Methodology

In this work formation of molecular halogens from the interaction of gaseous O_3 or OH with NaCl or NaBr aerosol particles is analyzed. In the past decade a number of models have been developed to study the chemistry of sea-salt aerosols.[2,3,40,44,62−67] MAGIC 2.0, the model used in this study, was developed initially to simulate the evolution of chemical species in the gas and aqueous phases for reactions of NaCl and NaBr particles in an aerosol chamber. This model includes a comprehensive treatment of gas-phase, aqueous-phase, and interfacial chemistry. A complete description of the chamber design, the experiments, and the model is found elsewhere.[2,3,63,68,69]

Processes occurring at the liquid−vapor interface are still not well understood, particularly with respect to their importance compared to bulk aqueous-phase processes. The main goal of this work is to analyze in detail the influence of interface reactions for NaBr and NaCl aerosols exposed to O_3 in the absence and presence of light and, in particular, to probe when interface reactions are important and when they are not. The following three interface processes are considered

$$Cl^-_{(surf)} + OH_{(g)} \rightarrow [\cdots] \rightarrow \frac{1}{2}Cl_{2(g)} + OH^-_{(surf)} \quad (5)$$

$$Br^-_{(surf)} + OH_{(g)} \rightarrow [\cdots] \rightarrow \frac{1}{2}Br_{2(g)} + OH^-_{(surf)} \quad (6)$$

$$Br^-_{(surf)} + O_{3(g)} \rightarrow [\cdots] \rightarrow \frac{1}{2}Br_{2(g)} + O_3^-_{(surf)} \quad (7)$$

where $Cl^-_{(surf)}$ and $Br^-_{(surf)}$ are halide ions available for reaction upon gas-phase oxidant collision with the aerosol surface. The detailed reaction mechanisms leading to Cl_2 or Br_2 are not known but clearly must involve several steps. In the absence of data regarding the individual steps, we represent the processes as overall reactions as shown in reactions 5−7.

To assess the viability of these processes, the enthalpy of each reaction, ΔH°_{rxn}, has been estimated using known gas- and aqueous-phase enthalpies of formation,[70,71] ΔH°_f. For reaction 7 an upper limit for the ΔH°_{rxn} was calculated using the available gas-phase ΔH°_f for O_3^-;[70] this will be an underestimate of the exothermicity since it does not take into account the enthalpy of solvation. All of the interface processes are predicted to be exothermic, with values of −57, −132, and −71 kJ/mol for reactions 5, 6, and 7, respectively.

The species included in MAGIC 2.0 are listed in Table 1. A total of 24 gas-phase species and 44 aqueous-phase species are included in the model. MAGIC 2.0 includes a detailed mathematical description of the physical and chemical processes occurring in the system. The concentration of chemical species changes according to

$$\frac{\partial C_g}{\partial t} = R_g \pm \omega R_{int} - \omega k_{mt} C_g + \frac{\omega k_{mt}}{HRT} C_{aq} \quad (I)$$

$$\frac{\partial C_{aq}}{\partial t} = R_{aq} \mp R_{int} + k_{mt} C_g + \frac{k_{mt}}{HRT} C_{aq} \quad (II)$$

C_g and C_{aq} represent the concentration in the gas and aqueous phase, respectively, and t denotes the time. R_g, R_{aq}, and R_{int} are the chemical reaction rates in the gas phase, aqueous phase, and interface, respectively. k_{mt} is the mass transfer coefficient. H represents the effective Henry's law constant, R is the universal gas constant, and T denotes absolute temperature (298 K). The volumetric aqueous aerosol liquid water mixing ratio (m^3 of water per m^3 of air) is represented by ω.

2.1. Interface Processes. Mass accommodation, or nonreactive uptake, and interface chemistry are inherently coupled processes. Interface reactions and uptake are modeled using a method similar to the treatment of Hu et al.[1] and Hanson[72] where the conventional resistor model[73,74] has been modified to take into account competition between surface reactions and mass accommodation. However, in the present case, the bulk-phase chemistry is treated explicitly rather than as a term in the resistor model.

Treatment of interface processes, including interface reactions and mass accommodation, is described below. Consider an ion X^- reacting at the surface with gas species A

$$X^-_{(surf)} + A_{(g)} \rightarrow [\cdots] \rightarrow \frac{1}{2}X_{2(g)} + A^-_{(surf)} \quad (8)$$

The interface rate, based on Schwartz's mass transfer model,[75] takes into account limitations due to gas-phase diffusion and reactant collisions at the surface. The interface reaction rate, expressed in terms of the aqueous-phase product formed, is defined by

$$R_{int} = \left(\frac{r^2}{3D_g} + \frac{4r}{3\upsilon\gamma}\right)^{-1} [A]_g \quad (III)$$

where

$$\gamma = \phi\gamma'\beta_X[X^-]_{aq} \quad (IV)$$

is the overall surface reaction probability, r is the aerosol radius,

and D_g is the gas-phase diffusion coefficient. The mean molecular speed of the colliding gas is represented by v. γ' denotes the probability that X^- and A react when these species collide, with allowed values from 0 and 1. The expression $\beta_X[X^-]_{aq}$ is the fraction of the droplet surface covered by the X^- halide ion estimated from molecular dynamics simulations[13] with a specific β_X parameter (with units of inverse concentration) for each sodium halide. This fraction is always significantly less than 1 so that γ does not exceed unity.

Molecular dynamics simulations[3,76] also suggest that OH and O_3 molecules approaching the surface of concentrated salt solutions experience multiple collisions with the surface halide species, a phenomenon that has been observed experimentally in other systems.[77] On the basis of these results, a parameter ϕ, which represents the average number of contacts between gas-phase reactants and surface halide ions, is now included in the overall reaction probability. The specific values chosen for β and ϕ are presented in the following section.

Recent papers[78−85] have disputed the validity of using the resistance model under some conditions, such as in flow-tube experiments. The standard resistance model is valid for systems with static, spherical boundary conditions and zero net flow, the conditions adopted in this study. In the present work it is assumed that there is no gas-phase resistance due to gas flow and that the particles are noninteracting, which hold for the aerosol chamber experiments used as the basis for these simulations.

To account for depletion of O_3 and OH at the interface due to reaction, the mass accommodation coefficient, α, is scaled accordingly. A molecule hitting the surface follows one of three paths: (1) bouncing off and returning to the gas phase, (2) reacting at the interface, or (3) being transferred to the drop, as indicated by the negative values of the mass transfer rate. Gas-phase species reacting at the surface should be removed from the total flux crossing the interface. This process is modeled in the mass transport coefficient, k_{mt}, by the following expression

$$k_{mt} = \left(\frac{r^2}{3D_g} + \frac{4r}{3v\alpha'}\right)^{-1} \quad \text{(V)}$$

where

$$\alpha' = \alpha(1 - \gamma) \quad \text{(VI)}$$

for O_3 and OH. For species not reacting at the surface, α' is equal to the standard mass accommodation coefficient, α, and eq V reduces to the Schwartz mass transfer model. If a gas molecule hits the drop, then preference is given to interface reactions using this approach. As discussed by Sander,[43] eq V assumes that mass transport changes from the continuum to the kinetic regime at the interface. However, the maximum error using this approach, even for a mass accommodation coefficient of 1, is less than 15%, and for computational efficiency eq V has been applied in these studies.

2.2. Aqueous-Phase Diffusion. Limitation of aqueous-phase reaction rates due to diffusion has been added using the equations developed by Schwartz and Freiberg.[75] The time for halide ions to diffuse from the bulk of these small particles into the interface region is short compared to the characteristic times for the interface reactions treated here, so that there is no significant depletion of the ions at the surface during the reaction.

2.3. Concentration Conversion. The molality (m) of highly concentrated NaCl and NaBr solutions is larger than the molarity (M) because the density is greater than 1 g cm^{-3}. Equations to determine thermodynamic quantities, such as activity coefficients and ionic strength, are given in terms of solution molality. Conversion of molarity to molality for the most concentrated species is now included in MAGIC using known densities for NaCl and NaBr solutions.[86−88]

TABLE 2: Model Parameters Used in the Simulations

parameter	NaCl	NaBr
aerosol median diameter (nm)	224	234
aerosol geometric standard deviation	1.7	1.9
aerosol concentration (cm^{-3})	1.9×10^5	2.5×10^5
relative humidity (%)	82	69
$[NaX]_0$ (M)	4.3	5.8
$[O_3]_0$ (ppm)	1.2	1.2
$[CO_2]_0$ (ppm)	0.96	0.96
β (M^{-1})	0.02	0.07
ϕ	3	2

3. Results and Discussion

Three interface processes are treated in the following sections: (1) $Cl^-_{(surf)}$ interacting with $OH_{(g)}$, (2) $Br^-_{(surf)}$ interacting with $OH_{(g)}$, and (3) $Br^-_{(surf)}$ interacting with $O_{3(g)}$. A detailed description of the aqueous- and gas-phase reactions included is found elsewhere.[3,63,89]

Snapshots of typical aqueous salt solution interfaces have been published elsewhere[2,3,11−14] and show that halide ions are readily available for reaction at the interface. Molecular dynamics results[13] predict that Cl^- occupies 12% of the surface area for a 6 M NaCl solution. Additionally, it is assumed that Br^- covers 42% of the surface area of a 6 M NaBr solution.[90] These results are used to define $\beta_{Cl} = 0.02$ and $\beta_{Br} = 0.07$, which are then assumed to apply to the slightly smaller concentrations of Cl^- and Br^- used in the model runs.

Molecular dynamics simulations[3,76] show that when gases such as O_3 and OH strike the surface of an aqueous halide solution, they have a finite residence time that increases the effective number of contacts with the halide ion compared to an elastic collision. On the basis of these molecular dynamics calculations, we estimate that the average number of contacts between gas-phase reactants and surface halide ions is approximately 2−3. To ensure that the overall surface reaction probability, γ, has an upper limit of 1 for both NaCl and NaBr, the average number of contacts per collision (ϕ) is taken to be 3 for Cl^- and 2 for Br^-.

At a typical chamber relative humidity of 82%, the initial NaCl concentration in the aerosol is 4.3 M.[63] For NaBr aerosols at 69% relative humidity, the initial NaBr concentration is 5.8 M.[3] Initial O_3 and CO_2 concentrations as well as particle size were chosen to be representative of prior chamber experiments[3,63] These parameters are shown in Table 2. Chamber conditions are adopted in the simulations because this controlled environment facilitates analysis and identification of the main chemical and physical processes occurring in and on the surface of sea-salt aerosols. This also allows for clear differentiation between surface and bulk halogen production from NaCl and NaBr aerosols.

3.1. Modeling $Cl^-_{(surf)} + OH_{(g)}$. Assuming 224 nm diameter particles and an aerosol concentration of 1.9×10^5 cm^{-3}, simulations for five interface reaction probabilities are presented. The interface reaction used for this case is shown in reaction 5. Figures 1a and 1b show the concentrations of Cl_2 and O_3 in the gas phase as a function of γ'. Note that for $\gamma' = 1$, 26% of the molecules that strike the surface of the aerosol result in reaction because the coverage of the surface by chloride is not complete. Although differences in the ozone decay rate are small, γ' does influence the level of molecular chlorine in the gas phase

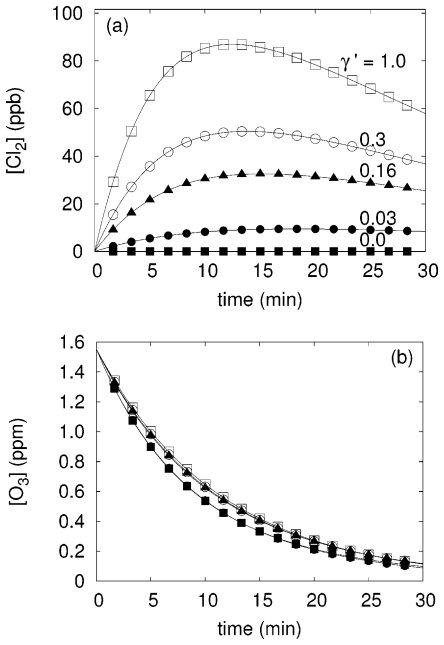

Figure 1. Predicted gas-phase Cl_2 and O_3 as a function of γ' for the NaCl + OH case. ■ $\gamma' = 0.0$; ● $\gamma' = 0.03$; ▲ $\gamma' = 0.16$; ○ $\gamma' = 0.3$; □ $\gamma' = 1.0$. See text for the definition of γ'.

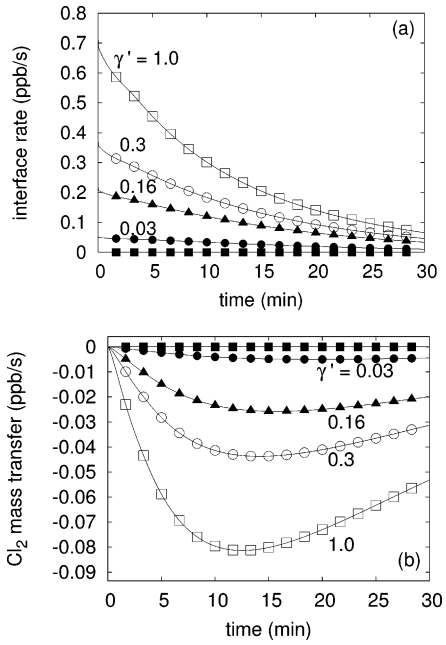

Figure 2. Predicted interface reaction rate and Cl_2 mass transfer from the drop as a function of γ' for the NaCl + OH case. A negative mass transfer rate corresponds to net flux toward the aqueous phase. ■ $\gamma' = 0.0$; ● $\gamma' = 0.03$; ▲ $\gamma' = 0.16$; ○ $\gamma' = 0.3$; □ $\gamma' = 1.0$. See text for the definition of γ'.

considerably. For the largest γ', $Cl_{2(g)}$ peak concentrations are more than 10^3 times larger than those predicted with no reaction at the surface.

Takami and et al.[91] suggest that the mass accommodation coefficient for OH is ≥ 0.01 and could approach unity. On the basis of these experiments, the mass accommodation coefficient for OH used in the model is $\alpha = 0.1$. Molecular dynamics simulations[15,92] suggest an upper limit for the mass accommodation coefficient of OH is $\alpha = 0.83$. Additional simulations have been performed to test the sensitivity of model results to the OH mass accommodation coefficient. Variation of this parameter between $\alpha = 0.01$ and $\alpha = 0.83$ leads to differences of less than 10% in results for all γ' values.

Cl_2 mass transfer from the gas to the aqueous phase and Cl_2 production at the interface are shown in Figures 2a and 2b, respectively. For nonzero values of γ', the interface reaction is the dominant pathway for production of gas-phase molecular chlorine. Gas-phase Cl_2 produced by the interface reaction is transferred to the drop. For $\gamma' = 0$, there is a small (not observable in Figure 2b) positive net flux of Cl_2 formed in the aqueous phase across the interface to the gas phase. However, the magnitude is small compared to the flux to the drop for nonzero values of γ'.

The interface reaction increases the pH to values higher than 11 due to the production of OH^-. When no interface reaction is considered, the pH rises rapidly and then remains constant at around 9.5, as shown in Figure 3. The pH increases, even without the presence of an interface reaction, because the $HOCl^-$ complex formed from $OH + Cl^-$ in the drop reacts with Cl^- to form OH^- and Cl_2^-. Under the conditions modeled here, which are representative of aerosol chamber experiments, the OH concentrations are high relative to the atmosphere, and this enhances the production of $HOCl^-$ in the particles.

Atmospheric particles have a lower pH than the pure NaCl aerosols considered here due to the uptake of acids and changes in pH due to chemistry in the aerosol droplets, such as the oxidation of S(IV) to S(VI). Higher H^+ concentrations would result in faster Cl_2 production in the aqueous phase via the general-acid-assisted reverse hydrolysis of $HOCl + Cl^-$.[93] Under

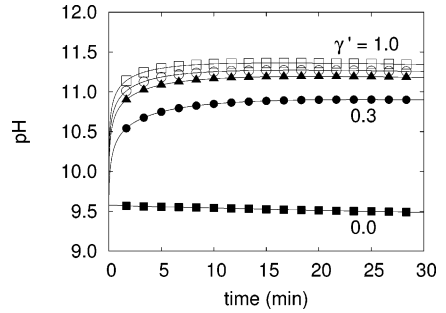

Figure 3. Predicted pH as a function of γ' for the NaCl + OH case. ■ $\gamma' = 0.0$; ● $\gamma' = 0.03$; ▲ $\gamma' = 0.16$; ○ $\gamma' = 0.3$; □ $\gamma' = 1.0$. See text for the definition of γ'.

atmospheric conditions, the surface reaction will occur in parallel with acidification of the particles, slowing down the rate of acidification compared to the case where there is no interface chemistry.

Several studies[94,95,116] suggest that H^+ is enhanced at the interface. However, H^+ concentrations at the interface cannot be responsible for production of $Cl_{2(g)}$ in this system. The particles begin as neutral and become more basic over time, so that the droplets never have a bulk H^+ concentration of more than 10^{-7} M. For the particle size considered here, this corresponds to less than 1 H^+ inside the volume of each droplet at neutral pH. Any protons present at the interface are rapidly titrated out by the OH^- produced via the interface reaction and cannot play a central role in the interface mechansim.

In short, the model results confirm the importance of interface processes for NaCl aerosol interacting with OH. The production of $Cl_{2(g)}$ at the interface is the dominant pathway when aerosols are not sufficiently acidic for the acid-catalyzed bulk chemistry to proceed at a significant rate.

3.2. Modeling $Br^-_{(surf)} + OH_{(g)}$. Parameters for simulations of the interaction of pure NaBr particles and OH formed by O_3 photolysis are shown in Table 2. The interface reaction for this case, reaction 6, is considered at five different γ' values. The

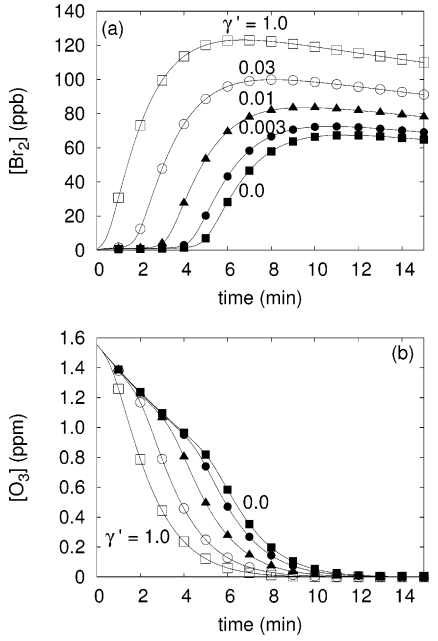

Figure 4. Predicted gas-phase Br_2 and O_3 as a function of γ' for the NaBr + OH case. ■ $\gamma' = 0.0$; ● $\gamma' = 0.003$; ▲ $\gamma' = 0.01$; ○ $\gamma' = 0.03$; □ $\gamma' = 1.0$. See text for the definition of γ'.

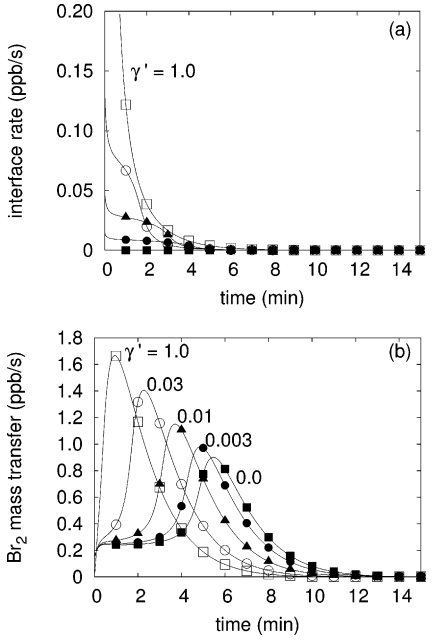

Figure 5. Predicted interface reaction rate and Br_2 mass transfer from the drop as a function of γ' for the NaBr + OH case. A positive mass transfer rate corresponds to net flux toward the gas phase. ■ $\gamma' = 0.0$; ● $\gamma' = 0.003$; ▲ $\gamma' = 0.01$; ○ $\gamma' = 0.03$; □ $\gamma' = 1.0$. See text for the definition of γ'.

aqueous-phase chemistry of Br^- differs from Cl^- because bromide is more readily oxidized than chloride and its oxidation occurs at a significant rate under less acidic conditions.

Figure 4a shows the influence of γ' on gas-phase Br_2 concentrations. With no interface reaction, the concentration of molecular bromine in the gas phase is negligible during the first 4 min of simulation. Predicted levels rise to a maximum of more than 65 ppb after 8 min, followed by slow Br_2 decay.

When an interface reaction is included, the peak in the gas-phase Br_2 is higher, reaching a maximum above 120 ppb for $\gamma' = 1$. In addition, the peak in the gas-phase Br_2 occurs earlier, reaching ppb levels in the first minute for the maximum interface reaction probability.

In contrast to the chlorine case, the bromine interface chemistry significantly impacts gas-phase ozone concentrations. For $\gamma' = 1$, half of the gas-phase O_3 is depleted after 2 min, as shown in Figure 4b. The mechanism for ozone decay is similar to ozone depletion episodes in the Arctic (for example, reactions 1−4), where increased Br_2 is correlated with ozone loss.[59]

Figure 5a illustrates that gas-phase Br_2 produced at the surface is only significant during the first several minutes and only for large values of γ' (>0.03). As shown by the positive values of the mass transfer rates in Figure 5b, Br_2 is transferred from the drop to the gas phase for all γ' values. This is a key difference from the chlorine case, where the net flux of was from the gas phase into the particles. For NaBr aerosols, the interface reaction competes with the aqueous-phase formation of Br_2 followed by mass transfer to the gas phase only in the initial stages of the reaction.

The are two main paths for Br_2 formation in the aqueous phase. First, the water-assisted reaction of Br^- and O_3 forms HOBr and OH^-.[3,96−98] HOBr then reacts with Br^- in solution to form molecular bromine.

$$Br^- + O_3 + H_2O \rightarrow HOBr + O_2 + OH^- \quad (9)$$

$$HOBr + Br^- \rightarrow OH^- + Br_2 \quad (10)$$

OH formed from photochemistry provides an additional aqueous-phase pathway for Br_2 production in the aerosol[37,99−101]

$$Br^- + OH \rightarrow OH^- + Br \quad (11)$$

$$Br + Br^- \rightarrow Br_2^- \quad (12)$$

$$Br_2^- + HO_2 \rightarrow Br_2 + HO_2^- \quad (13)$$

$$Br_2^- + Br_2^- \rightarrow Br_2 + 2Br^- \quad (14)$$

Aqueous-phase reactions 9−11 increase the alkalinity of the drops. The particles become basic over time even when there is no interface chemistry. The aerosol pH eventually approaches the same level, above 11, for all γ' values (Figure 6). The presence of hydroperoxy radicals and peroxide keeps the pH near 10.5, because they are both weak acids.[102−104]

$$HO_2 \leftrightarrow O_2^- + H^+ \quad (15)$$

$$(K_{a,298} = 2.05 \times 10^{-5}\ M)$$

$$H_2O_2 \leftrightarrow HO_2^- + H^+ \quad (16)$$

$$(K_{a,\,298} = 2.50 \times 10^{-12}\ M)$$

When O_3 is depleted, HO_2 and H_2O_2 concentrations decline, and the particles quickly become more basic. In addition to aqueous-phase chemistry, the interface reaction produces OH^- in the drop, contributing to increased aerosol alkalinity. The necessary time to achieve the maximum pH depends on the interface reaction probability. In contrast to the chlorine case, the interface reaction does not determine the pH at longer reaction times.

Results shown in Figures 4−6 are based on a mass accommodation coefficient for OH of $\alpha = 0.1$. Molecular dynamics suggest this value could be as large as 0.83,[15,92] as discussed in the previous section. To test the influence of a higher mass

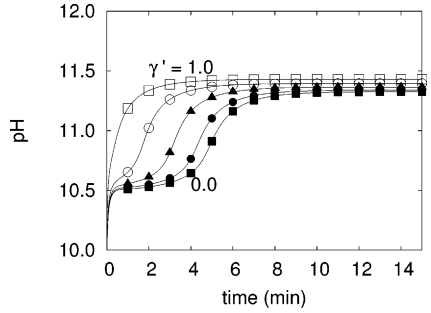

Figure 6. Predicted pH as a function of γ' for the NaBr + OH case. ■ $\gamma' = 0.0$; ● $\gamma' = 0.003$; ▲ $\gamma' = 0.01$; ○ $\gamma' = 0.03$; □ $\gamma' = 1.0$. See text for the definition of γ'.

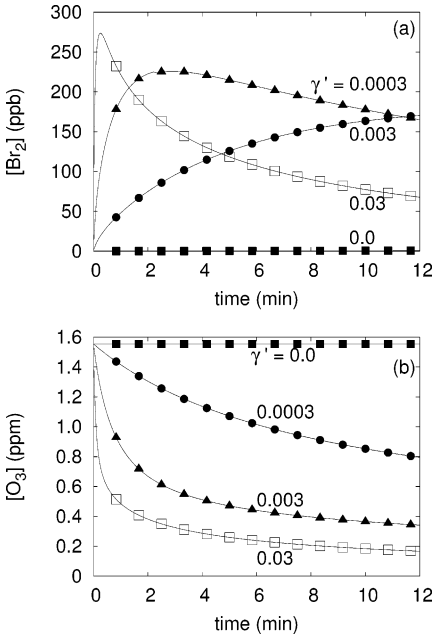

Figure 7. Predicted gas-phase Br_2 and O_3 as a function of γ' for the NaBr + O_3 case. ■ $\gamma' = 0.0$; ● $\gamma' = 0.0003$; ▲ $\gamma' = 0.003$; □ $\gamma' = 0.03$. See text for the definition of γ'.

accommodation coefficient on model results, calculations were also carried out for $\alpha = 0.83$. Under these conditions, OH is taken up into the bulk even more rapidly, further enhancing the importance of the bulk aqueous-phase chemistry. In this case, the results for $\gamma' \leq 0.03$ approach the data shown for $\gamma' = 1$.

For NaBr interacting with OH, aqueous-phase chemistry followed by mass transport is the main source of gas-phase Br_2. In brief, the interface reaction affects the system but is not the main pathway for gas-phase Br_2 production.

3.3. Modeling $Br^-_{(surf)}$ + $O_{3(g)}$. Unlike chloride,[105,106] bromide is oxidized at a significant rate by O_3 in the dark.[107−110] Recent aerosol chamber studies show that O_3 not only reacts with Br^- ions in the bulk but also at the interface.[3] This section analyzes the interface reaction between gas-phase O_3 and surface Br^- to form gas-phase Br_2 in the dark, reaction 7. The parameters used in this case are summarized in Table 2.

Due to the gradient in the interface reaction rate during the first seconds, computing γ' values above 0.03 results in a stiff differential equation system. However, values of γ' below 0.03 are a good representation of realistic interface reaction probabilities.[3]

Gas-phase Br_2 levels increase when the interface reaction is included in the model. For the highest γ' values, a Br_2 peak occurs during the few first seconds (Figure 7a), and the interface reaction rapidly depletes gas-phase ozone, Figure 7b. Ozone

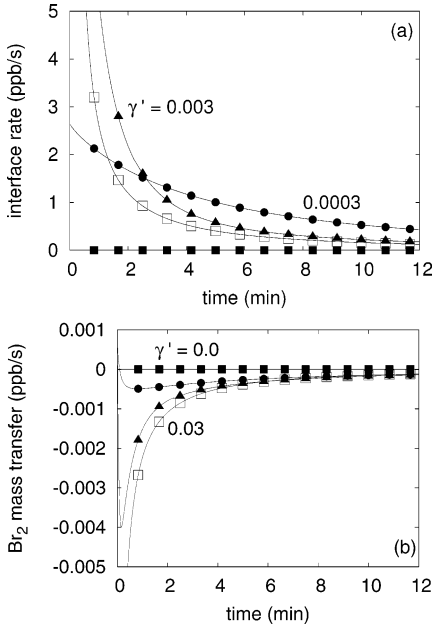

Figure 8. Predicted interface reaction rate and Br_2 mass transfer from the drop as a function of γ' for the NaBr + O_3 case. A negative mass transfer rate corresponds to net flux toward the aqueous phase. ■ $\gamma' = 0.0$; ● $\gamma' = 0.0003$; ▲ $\gamma' = 0.003$; □ $\gamma' = 0.03$. See text for definition of γ'.

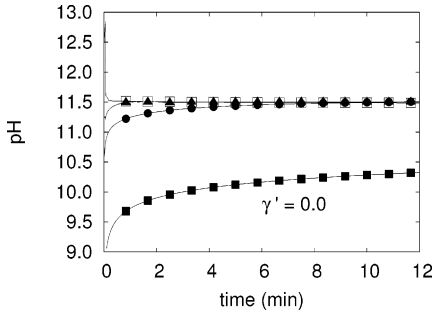

Figure 9. Predicted pH as a function of γ' for the NaBr + O_3 case. ■ $\gamma' = 0.0$; ● $\gamma' = 0.0003$; ▲ $\gamma' = 0.003$; □ $\gamma' = 0.03$. See text for definition of γ'.

depletion is negligible when no interface reaction is included. For $\gamma' = 0.03$, gaseous Br_2 is formed quickly and then taken up into the drop where it is hydrolyzed. When O_3 is completely depleted, no additional Br_2 is formed at the interface. To match $Br_{2(g)}$ observed by Hunt et al.,[3] an interface reaction probability of approximately 10^{-6} was used. This value accurately reproduces experimental results using MAGIC 2.0. A wider range of γ' values has been analyzed in this study to understand the relationship between aqueous-phase and interfacial chemistry.

In these simulations we used a value for the mass accommodation for O_3 of $\alpha = 0.002$, the recommended lower limit[49] based on the work of Utter et al.[111] Molecular dynamics simulations[92] suggest an upper limit of 0.047 for the ozone mass accommodation coefficient. Additional modeling runs with $\alpha = 0.047$ for ozone showed no observable difference compared to $\alpha = 0.002$.

For intermediate γ' values, Br_2 forms more slowly. However, the concentration is higher at long times because less Br_2 is taken up into the drop and lost due to hydrolysis. There are two reasons why this occurs. First, with higher interface reaction rates, gas-phase Br_2 is produced by the interface reaction very quickly and transferred to the drop (Figures 8a and 8b). Second, high interface reaction rates result in an initial peak in pH. As

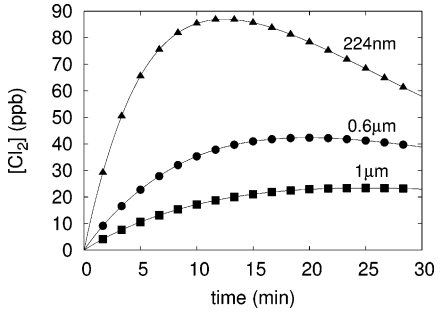

Figure 10. Predicted $Cl_{2(g)}$ for several different particle sizes with constant liquid water content. ■ diameter = 1 μm; ● diameter = 0.6 μm; ▲ diameter = 224 nm.

a consequence, the rate of Br_2 hydrolysis in the drop increases

$$Br_2 + OH^- \rightarrow HOBr + Br^- \qquad (17)$$

As shown in reactions 9 and 10, HOBr is an essential intermediate needed to form Br_2 from aqueous-phase chemistry. However, at high pH values, HOBr ($K_{a,298} = 1.58 \times 10^{-9}$ M)[112] primarily exists as OBr^- and does not contribute to the formation of Br_2 in the aqueous phase.

At intermediate interface reaction rates, ozone is available for interface processes for a longer period of time, the Br_2 mass transfer is slower, and there is no spike in pH. As a result, the concentration of Br_2 at long reaction times is higher than in cases with high or low interface reaction probabilities.

The pH of the particles is influenced by the interface reaction, as shown in Figure 9. For $\gamma' = 0$, the pH increases slowly to a maximum of 10.2. For the other cases, the pH reaches 11.5 rapidly due to O_3^- production at the interface. Surface O_3^- is transferred to the bulk and decays to O_2 and O^-, which reacts with water to form OH^-, increasing aerosol pH.

In summary, as in the OH + $Cl^-_{(surf)}$ reaction, interface chemistry is predicted to be the main source of gas-phase Br_2.

3.4. Particle Size. The influence of particle size on halogen production is clearly a key parameter in understanding the relative importance of aqueous-phase versus interface chemistry. Small particles have a relatively large surface-to-volume ratio when compared with larger aerosols. Therefore, interface chemistry should be most important for the smallest aerosols. Modeling aerosols of different sizes is important to understand the trends as particle size increases.

Figure 10 shows the predicted concentration of $Cl_{2(g)}$, with $\gamma' = 1$ for the Cl^- + OH interface reaction, for three different aerosol diameters (224 nm, 0.6 μm, and 1 μm). Model conditions, other than particle size and concentration, are those in Table 2. The liquid water content (LWC), or total aqueous volume per m^3 of air, has been held constant by varying the particle concentration. This has been done to ensure similar contributions from aqueous-phase chemistry for all particle sizes. Since the surface-to-volume ratio varies with the inverse of the particle radius, the total surface area also scales with r^{-1} at constant volume. As expected, as the aerosol diameter increases, the total amount of Cl_2 produced from the interface reaction decreases. In addition, the gas-phase diffusion limitation becomes more important as the size increases and reduces the reaction rate by about 35% for 1 μm particles. The contribution from aqueous-phase chemistry is negligible for all particle sizes, confirming that the interface reaction remains an important pathway for halogen production even for larger aerosols. Without the interface reaction, $\gamma' = 0$, the concentration of gas-phase Cl_2 remains almost zero for all diameters. Under these conditions, the aqueous-phase chemistry to form Cl_2 does not proceed at a significant rate, independent of particle size.

4. Conclusions

This study has quantified the relative importance of interface and bulk-phase chemistry in the reactions of OH and O_3 with deliquesced NaCl and NaBr particles and provides insight into the factors that govern their relative importance. The most obvious factor is the size of the particles for a fixed liquid water content. The smaller the particles, the greater the surface-to-volume ratio, and the relatively more important is interface chemistry. The gas-phase diffusion limitation is also negligible for smaller particles (although this affects both interface and bulk-phase chemistry equally). This was the case in earlier chamber studies of sea-salt chemistry where particles with diameters of ~100−200 nm were used.[2,3,68]

The most important factor is shown to be whether there is rapid bulk-phase chemistry that can compete with the interface reaction. In the case of the Cl^- oxidation by OH, the bulk-phase chemistry is acid-catalyzed. In the absence of an acid, this is sufficiently slow that the interface reaction dominates by several orders of magnitude. It is important that the interface reaction does not require an acid; indeed the reaction actually generates hydroxide ions.[113] However, the bulk aqueous-phase oxidation of Br^- by OH is sufficiently fast starting at neutral pH that the interface reaction only contributes for large reaction probabilities and at short reaction times before the chain chemistry such as that in reactions 1−4 takes over. Finally, the production of gas-phase Br_2 through the oxidation of Br^- by O_3 has significant contributions from both the interface reaction and from bulk aqueous-phase reactions.

Modeling aqueous-phase chemistry and mass transfer processes for system with high ionic strength remains challenging. Future work to understand how reaction rates scale with ionic strength is needed. In addition, mass transfer between the gas and aqueous phase could be modeled more accurately if Setchenov coefficients were available for a wide variety of gas-phase species at a variety of ionic strengths.

It is challenging to extend the results from kinetics box model studies to real atmospheric aerosols. However, understanding the sensitivity of pure NaCl and NaBr aerosols to interface reaction probability under chamber conditions is the first step in analyzing how interface reactions contribute to molecular halogens in the troposphere. Processes occurring both in and on atmospheric sea-salt aerosols are extremely complex and a complete understanding of how interface reactions impact the overall chemistry of these particles is still needed.

However, the present results suggest that interface chemistry is more likely to be important for chloride ion reactions than for bromide, given the rapid bulk-phase chemistry of Br^-, recycling between the gas and aqueous/solid phases represented by reactions such as 1−4 and the molar ratio of Cl^-/Br^- in sea salt of ~650:1. The exception is likely to be the reaction of O_3 with Br^-, which has been hypothesized[56,114] to initiate the chain reactions that lead to ozone loss in the Arctic at polar sunrise. Given the important contribution of the reaction of ozone at the interface with bromide ions suggested by these model studies, by experimental studies of NaBr aerosols at room temperature,[3] and by recent data showing enhancement of bromide ions at the air−water interface,[115] the interface reaction may be a key to this unusual chemistry. It also suggests that key atmospheric reactions of bromide ions with other trace gases such as HOBr should be explored for a contribution from interface chemistry. In addition, studies that treat the chemistry,

physical processes, and molecular dynamics of particles whose composition reflects the complexity of sea salt are clearly warranted.

Acknowledgment. This work was supported by the National Science Foundation (Grant Nos. 0209719 and 0431312). J.L.T. and A.J.A. were partially supported by the U. S. Civilian Research and Development Foundation (Grant No. RC2-2521-MO-03) and the Balsells-Generalitat de Catalunya Fellowship Program, respectively. We are also grateful to all of the members of AirUCI for assistance, in particular Douglas Tobias, Lisa M. Wingen, Martina Roeselová, Eladio M. Knipping, Sherri W. Hunt, and Pavel Jungwirth for helpful discussions.

References and Notes

(1) Hu, J. H.; Shi, Q.; Davidovits, P.; Worsnop, D. R.; Zahniser, M. S.; Kolb, C. E. *J. Phys. Chem.* **1995**, *99*, 8768−8776.

(2) Knipping, E. M.; Lakin, M. J.; Foster, K. L.; Jungwirth, P.; Tobias, D. J.; Gerber, R. B.; Dabdub, D.; Finlayson-Pitts, B. J. *Science* **2000**, *288*, 301−306.

(3) Hunt, S. W.; Roeselová, M.; Wang, W.; Wingen, L. M.; Knipping, E. M.; Tobias, D. J.; Dabdub, D.; Finlayson-Pitts, B. J. *J. Phys. Chem. A* **2004**, *108*, 11559−11572.

(4) Benjamin, I. *J. Chem. Phys.* **1991**, *95*, 3698−3709.

(5) Wilson, M. A.; Pohorille, A. *J. Chem. Phys.* **1991**, *95*, 6005−6013.

(6) Dang, L. X.; Garrett, B. C. *J. Chem. Phys.* **1993**, *99*, 2972−2977.

(7) Dang, L. X.; Smith, D. E. *J. Chem. Phys.* **1993**, *99*, 6950−6956.

(8) Stuart, S. J.; Berne, B. J. *J. Phys. Chem.* **1996**, *100*, 11934−11943.

(9) Stuart, S. J.; Berne, B. J. *J. Phys. Chem. A.* **1999**, *103*, 10300−10307.

(10) Dang, L. X. *J. Chem. Phys.* **1999**, *110*, 1526−1532.

(11) Jungwirth, P.; Tobias, D. J. *J. Phys. Chem. B* **2000**, *104*, 7702−7706.

(12) Jungwirth, P.; Tobias, D. J. *J. Phys. Chem. B* **2001**, *105*, 10468−10472.

(13) Jungwirth, P.; Tobias, D. J. *J. Phys. Chem. B* **2002**, *106*, 6361−6373.

(14) Jungwirth, P.; Tobias, D. J. *J. Phys. Chem. A* **2002**, *106*, 1286−1298.

(15) Roeselová, M.; Vieceli, J.; Dang, L. X.; Garrett, B. C.; Tobias, D. J. *J. Am. Chem. Soc.* **2004**, *126*, 16308−16309.

(16) Vácha, R.; Slavícek, P.; Mucha, M.; Finlayson-Pitts, B. J.; Jungwirth, P. *J. Phys. Chem. A* **2004**, *108*, 11573−11579.

(17) Jayne, J. T.; Davidovits, P.; Worsnop, D. R.; Zahniser, M. S.; Kolb, C. E. *J. Phys. Chem.* **1990**, *94*, 6041−6048.

(18) Hanson, D. R.; Ravishankara, A. R. *J. Phys. Chem.* **1994**, *98*, 5728−5735.

(19) Donaldson, D. J.; Guest, J. A.; Goh, M. C. *J. Phys. Chem.* **1995**, *99*, 9313−9315.

(20) George, C.; Behnke, W.; Sheer, V.; Zetzsch, C.; Magi, L.; Ponche, J. L.; Mirabel, P. *Geophys. Res. Lett.* **1995**, *22*, 1505−1508.

(21) Boniface, J.; Shi, Q.; Li, Y. Q.; Cheung, J. L.; Rattigan, O. V.; Davidovits, P.; Worsnop, D. R.; Jayne, J. T.; Kolb, C. E. *J. Phys. Chem. A* **2000**, *104*, 7502−7510.

(22) Clegg, S. M.; Abbatt, J. P. D. *J. Phys. Chem. A* **2001**, *105*, 6630−6636.

(23) Katrib, Y.; Diber, G.; Schweitzer, F.; Mirabel, P.; George, C. *J. Aerosol Sci.* **2001**, *32*, 893−911.

(24) Strekowski, R. S.; Remorov, R.; George, C. *J. Phys. Chem. A* **2003**, *107*, 2497−2504.

(25) Mmereki, B. T.; Donaldson, D. J.; Gilman, J. B.; Eliason, T. L.; Vaida, V. *Atmos. Environ.* **2004**, *38*, 6091−6103.

(26) Finlayson-Pitts, B.; Pitts, J. N. *Chemistry of the Upper and Lower Atmosphere*; Academic Press: San Diego, CA, 2000.

(27) Stutz, J.; Hebestreit, K.; Alicke, B.; Platt, U. *J. Atmos. Chem.* **1999**, *34*, 65−85.

(28) Hebestreit, K.; Stutz, J.; Rozen, D.; Matveiv, V.; Peleg, M.; Luria, M.; Platt, M. *Science* **1999**, *283*, 55−57.

(29) Matveev, V.; Peleg, M.; Rosen, D.; Tov-Alper, D. S.; Hebestreit, K.; Stutz, J.; Blake, D.; Luria, M. *J. Geophys. Res.* **2001**, *106*, 10375−10388.

(30) Tas, E.; Peleg, M.; Matveev, V.; Zingler, J.; Luria, M. *J. Geophys. Res.* **2005**, *110*, doi: 10.1029/2004JD005665.

(31) Stutz, J.; Ackermann, R.; Fast, J. D.; Barrie, L. *Geophys. Res. Lett.* **2002**, *29*, 1380, doi: 10.1029/2002GL014812.

(32) Andreae, M. O.; Crutzen, P. J. *Science* **1997**, *276*, 1052−1058.

(33) Finlayson-Pitts, B. J.; Pitts, J. N. *Science* **1997**, *276*, 1045−1052.

(34) Ravishankara, A. R. *Science* **1997**, *276*, 1058−1065.

(35) Hemminger, J. C. *Int. Rev. Phys. Chem.* **1999**, *18*, 387−417.

(36) Finlayson-Pitts, B. J.; Hemminger, J. C. *J. Phys. Chem. A* **2000**, *104*, 11463−11477.

(37) Anastasio, C.; Mozurkewich, M. *J. Atmos. Chem.* **2002**, *41*, 135−162.

(38) Rossi, M. J. *Chem. Rev.* **2003**, *103*, 4823−4882.

(39) Finlayson-Pitts, B. J. *Chem. Rev.* **2003**, *103*, 4801−4822.

(40) Sander, R.; Crutzen, P. J. *J. Geophys. Res.* **1996**, *101*, 9121−9138.

(41) Keene, W. C. Inorganic Cl Cycling in the Marine Boundary Layer: A Review. In *Naturally-Produced Organohalogens*; Kluwer Academic Publishers: Boston, MA, 1995.

(42) Keene, W. C.; Sander, R.; Pszenny, A. A. P.; Vogt, R.; Crutzen, P. J.; Galloway, J. N. *J. Aerosol Sci.* **1998**, *29*, 339−356.

(43) Sander, R. *Surv. Geophys.* **1999**, *20*, 1−31.

(44) Moldanová, J.; Ljungström, E. *J. Geophys. Res.* **2001**, *106* (D1), 1271−1296.

(45) Herrmann, H.; Majdik, Z.; Ervens, B.; Weise, D. *Chemosphere* **2003**, *52*, 485−502.

(46) Knipping, E. M.; Dabdub, D. *Environ. Sci. Technol.* **2003**, *37*, 275−284.

(47) Atkinson, R. *J. Phys. Chem. Ref. Data* **1997**, *26*, 215−290.

(48) Atkinson, R.; Baulch, D. L.; Cox, R. A.; Hampson, R. F.; Kerr, J. A.; Rossi, M. J.; Troe, J. *J. Phys. Chem. Ref. Data* **2000**, *29*, 167−266.

(49) Sander, S. P.; Ravishankara, A. R.; Friedl, R. R.; Golden, D. M.; Kolb, C. E.; Kurylo, M. J.; Molina, M. J.; Huie, R. E.; Orkin, V. L.; Moortgat, G. K.; Finlayson-Pitts, B. J. *Chemical Kinetics and Photochemical Data for Use in Atmospheric Studies*; Technical Report, Evaluation Number 14; Jet Propulsion Laboratory: Pasadena, CA, 2003.

(50) Barrie, L. A.; Bottenheim, J. W.; Schnell, R. C.; Crutzen, P. J.; Rasmussen, R. A. *Nature* **1988**, *334*, 138−141.

(51) Finlayson-Pitts, B. J.; Livingston, F. E.; Berko, H. N. *Nature* **1990**, *343*, 622−625.

(52) Bottenheim, J. W.; Barrie, L. A.; Atlas, E.; Heidt, L. E.; Niki, H.; Rasmussen, R. A.; Shepson, P. B. *J. Gephys. Res.* **1990**, *95*, 18555−18568.

(53) Fan, S. M.; Jacob, D. J. *Nature* **1992**, *359*, 522−524.

(54) McConnell, J. C.; Henderson, G. S.; Barrie, L.; Bottenheim, J.; Niki, H.; Langford, C. H.; Templeton, E. M. J. *Nature* **1992**, *355*, 150−152.

(55) Barrie, L.; Platt, U. *Tellus, Ser. B* **1997**, *49*, 450−454.

(56) Impey, G. A.; Shepson, P. B.; Hastie, D. R.; Barrie, L. A.; Anlauf, K. G. *J. Geophys. Res.* **1997**, *102*, 16005−16010.

(57) Impey, G. A.; Mihele, C. M.; Anlauf, K. G.; Barrie, L. A.; Hastie, D. R.; Shepson, P. B. *J. Atmos. Chem.* **1999**, *34*, 21−37.

(58) Lehrer, E.; Wagenbach, D.; Platt, U. *Tellus, Ser. B* **1997**, *49*, 486−495.

(59) Foster, K. L.; Plastridge, R. A.; Bottenheim, J. W.; Shepson, P. B.; Finlayson-Pitts, B. J.; Spicer, C. W. *Science* **2001**, *291*, 471−474.

(60) Spicer, C. W.; Plastridge, R. A.; Foster, K. L.; Finlayson-Pitts, B. J.; Bottenheim, J. W.; Grannas, A. M.; Shepson, P. B. *Atmos. Environ.* **2002**, *36*, 2721−2731.

(61) Platt, U.; Hönninger, G. *Chemosphere* **2003**, *53*, 325−338.

(62) Herrmann, H.; Ervens, B.; Jacobi, H. W.; Wolke, R.; Nowacki, P.; Zellner, R. *J. Atmos. Chem.* **2000**, *36*, 231−284.

(63) Knipping, E. M.; Dabdub, D. *J. Geophys. Res.* **2002**, *107*, 4360, doi: 10.1029/2001JD000867.

(64) von Glasow, R.; Sander, R.; Bott, A.; Crutzen, P. J. *J. Geophys. Res.* **2002**, *107*, 4341, doi: 10.1029/2001JD000942.

(65) von Glasow, R.; Sander, R.; Bott, A.; Crutzen, P. J. *J. Geophys. Res.* **2002**, *107*, 4323, doi: 10.1029/2001JD000943.

(66) Pszenny, A. A. P.; Moldanova, J.; Keene, W. C.; Sander, R.; Maben, J. R.; Martinez, M.; Crutzen, P. J.; Perner, D.; Prinn, R. G. *Atmos. Chem. Phys.* **2004**, *4*, 147−168.

(67) Keene, W. C.; Pszenny, A. A. P. *Science* **2004**, *303*, 628.

(68) Oum, K. W.; Lakin, M. J.; DeHaan, D. O.; Brauers, T.; Finlayson-Pitts, B. J. *Science* **1998**, *279*, 74−77.

(69) De Haan, D. O.; Brauers, T.; Oum, K. W.; Stutz, J.; Nordmeyer, T.; Finlayson-Pitts, B. J. *Int. Rev. Phys. Chem.* **1999**, *18*, 343−385.

(70) *NIST Standard Reference Database Number 69*; National Institute of Standards and Technology: Gaithersburg, MD, 2005. http://webbook.nist.gov/chemistry.

(71) *CRC Handbook of Chemistry and Physics*, 85th ed.; Lide, D. R., Ed.; CRC Press: Boca Raton, FL, 2005.

(72) Hanson, D. R. *J. Phys. Chem. B* **1997**, *101*, 4998−5001.

(73) Kolb, C. E.; Worsnop, D. R.; Zahniser, M. S.; Davidovits, P.; Keyser, L. F.; Leu, M. T.; Molina, M. J.; Hanson, D. R.; Ravishankara, A. R. Laboratory Studies of Atmospheric Heterogeneous Chemistry. In *Progress and Problems in Atmospheric Chemistry*; World Scientific: River Edge, NJ, 1995; Vol. 3.

(74) Kolb, C. E.; Jayne, J. T.; Worsnop, D. R.; Davidovits, P. *Pure Appl. Chem.* **1997**, *69*, 959−968.

(75) Schwartz, S. E. Mass Transport Considerations Pertinent to Aqueous Phase Reactions of Gases in Liquid-Water Clouds. In *Chemistry of Multiphase Atmospheric Systems*; NATO ASI Series G6; Springer-Verlag: New York, 1986.

(76) Roeselová, M.; Jungwirth, P.; Tobias, D. J.; Gerber, R. B. *J. Phys. Chem. B* **2003**, *107*, 12690−12699.
(77) Nathanson, G. M. *Annu. Rev. Phys. Chem.* **2004**, *55*, 231−255.
(78) Sugiyama, M.; Koda, S.; Morita, A. *Chem. Phys. Lett.* **2002**, *362* (1−2), 56−62.
(79) Morita, A.; Sugiyama, M.; Koda, S. *J. Phys. Chem. B.* **2003**, *107*, 1749.
(80) Davidovits, P.; Worsnop, D. R.; Jayne, J. T.; Kolb, C. E.; Winkler, P.; Vrtala, A.; Wagner, P. E.; Kulmala, M.; Lehtinen, K. E. J.; Vesala, T.; Mozurkewich, M. *Geophys. Res. Lett.* **2004**, *31*, L22111.
(81) Morita, A.; Sugiyama, M.; Kameda, H.; Koda, S.; Hanson, D. R. *J. Phys. Chem. B.* **2004**, *108*, 9111−9120.
(82) Morita, A.; Sugiyama, M.; Koda, S. *J. Phys. Chem. B.* **2004**, *108*, 8544−8545.
(83) Worsnop, D. R.; Williams, L. R.; Kolb, C. E.; Mozurkewich, M.; Gershenzon, M.; Davidovits, P. *J. Chem. Phys. A* **2004**, *108*, 8542−8543.
(84) Morita, A.; Sugiyama, M.; Koda, S.; Hanson, D. R. *J. Phys. Chem. B.* **2005**, *109*, 14747−14749.
(85) Davidovits, P.; Worsnop, D. R.; Williams, L. R.; Kolb, C. E.; Gerhenzon, M. *J. Phys. Chem. B.* **2005**, *109*, 14742−14746.
(86) Pitzer, K. S.; Peiper, J. C.; Busey, R. H. *J. Phys. Chem. Ref. Data* **1984**, *13*, 1−96.
(87) Cohen, M. D.; Flagan, R. C.; Seinfeld, J. H. *J. Phys. Chem.* **1987**, *91*, 4563−4574.
(88) Carper, J. *The CRC Handbook of Chemistry and Physics*; Chemical Rubber Publishing Co.: Boca Raton, FL, 1999.
(89) Knipping, E. M. Modeling Urban Coastal Chemistry. Ph.D. Thesis, University of California, Irvine, Irvine, CA, 2002.
(90) Tobias, D. J.; Roeselová, M. Personal communication.
(91) Takami, A.; Kato, S.; Shimono, A.; Koda, S. *Chem. Phys.* **1998**, *231*, 215−227.
(92) Vieceli, J.; Roeselová, M.; Potter, N.; Dang, L. X.; Garrett, B. C.; Tobias, D. J. *J. Phys. Chem. B* **2005**, *109*, 15876−15892.
(93) Wang, T. X.; Margerum, D. W. *Inorg. Chem.* **1994**, *33* (6), 1050−1055.
(94) Petersen, M. K.; Iyengar, S. S.; Day, T. J. F.; Voth, G. A. *J. Phys. Chem. B* **2004**, *108*, 14804−14806.
(95) Mucha, M.; Frigato, T.; Levering, L. M.; Allen, H. C.; Tobias, D. J.; Dang, L. X.; Jungwirth, P. *J. Phys. Chem. B* **2005**, *109*, 7617−7623.
(96) von Gunten, U.; Hoigné, J. *Environ. Sci. Technol.* **1994**, *28*, 1234−1242.
(97) Disselkamp, R. S.; Chapman, E. G.; Barchet, W. R.; Colson, S. D.; Howd, C. D. *Geophys. Res. Lett.* **1999**, *26*, 2183−2186.
(98) Liu, Q.; Schurter, L. M.; Muller, C. E.; Aloisio, S. Francisco, J. S.; Margerum, D. W. *Inorg. Chem.* **2001**, *40*, 4436−4442.
(99) *NIST Chemical Kinetics Database, NIST Standard Reference Database 17*, version 7.0; National Institute of Standards and Technology: Gaithersburg, MD, 2000.
(100) Mamou, A.; Rabani, J.; Behar, D. *J. Phys. Chem.* **1977**, *81*, 1447−1448.
(101) Mozurkewich, M. *J. Geophys. Res.* **1995**, *100*, 14199−14208.
(102) Bielski, B. H. J. *Photochem. Photobiol.* **1978**, *28*, 645−649.
(103) Sauer, M. C., J.; Brown, W. G.; Hart, E. J. *J. Phys. Chem.* **1984**, *88*, 1398−1400.
(104) Bielski, B. H. J.; Cabelli, D. E.; Arudi, R. L.; Ross, A. B. *J. Phys. Chem. Ref. Data* **1985**, *14*, 1041−1100.
(105) Yeatts, L. B., J.; Taube, H. *J. Am. Chem. Soc.* **1949**, *71*, 4100−4105.
(106) Hoigne, J.; Bader, H.; Haag, W.; Staehelin, J. *Water Res.* **1985**, *19*, 993−1004.
(107) Taube, H. *J. Am. Chem. Soc.* **1942**, *64*, 2468−2474.
(108) Garland, J.; Elzerman, A.; Penkett, S. *J. Geophys. Res., C* **1980**, *85*, 7488−7492.
(109) Haruta, K.; Takeyama, T. *J. Phys. Chem.* **1981**, *85*, 2383−2388.
(110) Haag, W. R.; Hoigne, J. *Environ. Sci. Technol.* **1983**, *17*, 261−267.
(111) Utter, R. G.; Burkholder, J. B.; Howard, C. J.; Ravishankara, A. R. *J. Phys. Chem.* **1992**, *96*, 4673−4979.
(112) Troy, R. C.; Margerum, D. W. *Inorg. Chem.* **1991**, *30*, 3538−3543.
(113) Laskin, A.; Gaspar, D. J.; Wang, W.; Hunt, S. W.; Cowin, J. P.; Colson, S. D.; Finlayson-Pitts, B. *Science* **2003**, *301*, 340−344.
(114) Oum, K. W.; Lakin, M. J.; Finlayson-Pitts, B. J. *Geophys. Res. Lett.* **1998**, *25*, 3923−3926.
(115) Ghosal, S.; Hemminger, J. C.; Bluhm, H.; Mun, B. S.; Hebenstreit, E. L. D.; Ketteler, G.; Ogletree, D. F.; Requejo, F. G.; Salmeron, M. *Science* **2005**, *307*, 563−566.
(116) Petersen, P. B.; Saykally, R. J. *J. Phys. Chem. B* **2005**, *109*, 7976−7980.